Predicting aviation non-volatile particulate matter emissions at cruise via convolutional neural network

Ge, Fudong; Yu, Zhenhong; Li, Yan; Zhu, Meiyin; Zhang, Bin; Zhang, Qian; Harrison, Roy M.; Chen, Longfei

DOI:
10.1016/j.scitotenv.2022.158089

Predicting Aviation Non-Volatile Particulate Matter Emissions at Cruise via Convolutional Neural Network

Fudong Ge [a,b], Zhenhong Yu [b], Yan Li [a,b], Meiyin Zhu [b], Bin Zhang [b], Qian Zhang [a],
Roy M. Harrison [c], Longfei Chen [a,b,*]

[a] School of Energy and Power Engineering, Beihang University, Beijing, 100191, China
[b] Beihang Hangzhou Innovation Institute Yuhang, Xixi Octagon City, Yuhang District, Hangzhou, 310023, China
[c] School of Geography, Earth & Environmental Sciences, University of Birmingham, Edgbaston, Birmingham, B15 2TT, UK

ABSTRACT

Aviation emissions are the only direct source of anthropogenic particulate pollution at high altitudes, which can form contrails and contrail-induced clouds, with consequent effects upon global radiative forcing. In this study, we develop a predictive model, called APMEP-CNN, for aviation non-volatile particulate matter (nvPM)

[*] Corresponding author.
E-mail address: chenlongfei@buaa.edu.cn (L. Chen).

emissions using a convolutional neural network (CNN) technique. The model is established with data sets from the newly published aviation emission databank and measurement results from several field studies on the ground and during cruise operation. The model also takes the influence of sustainable aviation fuels (SAFs) on nvPM emissions into account by considering fuel properties. This study demonstrates that the APMEP-CNN can predict nvPM emission index in mass (EI_m) and number (EI_n) for a number of high-bypass turbofan engines. The accuracy of predicting EI_m and EI_n at ground level is significantly improved ($R^2 = 0.96$ and 0.96) compared to the published models. We verify the suitability and the applicability of the APMEP-CNN model for estimating nvPM emissions at cruise and burning SAFs and blend fuels, and find that our predictions for EI_m are within ±36.4% of the measurements at cruise and within ±33.0% of the measurements burning SAFs in average. In the worst case, the APMEP-CNN prediction is different by -69.2% from the measurements at cruise for the JT3D-3B engine. Thus, the APMEP-CNN model can provide new data for establishing accurate emission inventories of global aviation and help assess the impact of aviation emissions on human health, environment and climate.

HIGHLIGHTS

- Application of convolutional neural network for aviation emission predictions.
- Good agreement on nvPM emissions at cruise between measurements and calculation.
- Capability of predicting nvPM emissions for aircrafts burning SAFs.

KEYWORDS

Aircraft engine, Aviation emission, Non-volatile particulate matter, Sustainable aviation fuel, Cruise, Convolutional neural network

SYNOPSIS

The results of this paper provide accurate predictions of nvPM emissions from in-use aircraft engines, which impact airport local air quality and global radiative forcing.

GRAPHICAL ABSTRACT

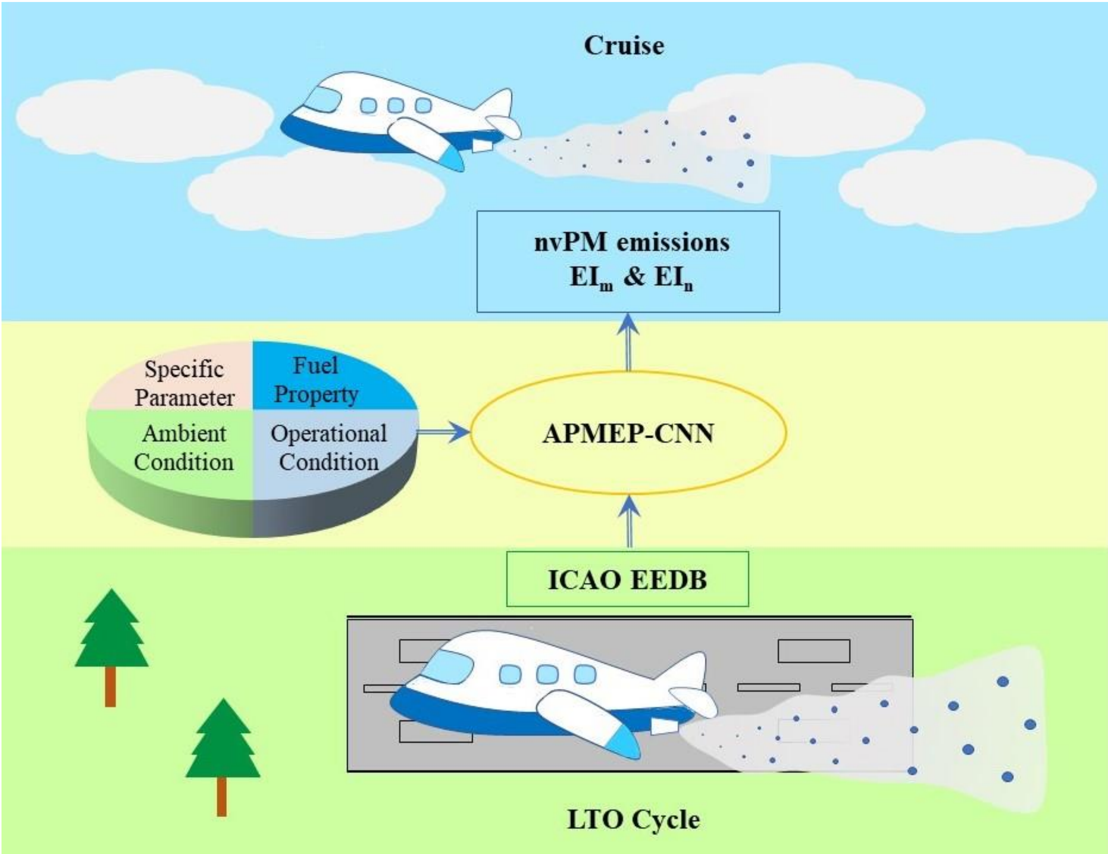

Cruise
nvPM emissions
EIm & EIn
Specific Parameter
Fuel Property
Ambient Condition
Operational Condition
APMEP-CNN
ICAO EEDB
LTO Cycle

1. INTRODUCTION

In the past twenty years, impacts from aviation emissions on human health, airport local air quality, and climate change have attracted increasing interest (Stettler et al., 2011; Yim et al., 2013; Yim et al., 2015). Non-volatile particulate matter (nvPM) as one of the major pollutants from aviation has been widely studied (Liati et al., 2014; Lobo et al., 2015; Lobo et al., 2016) and currently regulated in engine certification process by the International Civil Aviation Organization (ICAO) (ICAO, 2021). At present, aviation is the only anthropogenic source that emits nvPM at cruise altitude (~ 10,000 m) in the upper troposphere or lower stratosphere (Jensen and Toon, 1997; Peck et al., 2013). In fact, more than 90% of global aviation fuel is consumed at cruise altitude (Zhang et al., 2019).

Aviation nvPM, often assumed to be predominantly composed of black carbon (BC) or soot, has been widely considered as one of the major contributors to climate change (Lee et al., 2009; Lee et al., 2021). The nvPM emissions from aviation at cruise altitude can influence the global radiation balance via two mechanisms: (i) the direct absorption of solar radiation. The nvPM strongly absorbs solar light in the spectral range from ultraviolet to infrared (Lee et al., 2021). Additionally, compared to the nvPM emissions from other anthropogenic sources, nvPM from aviation emission has a long lifetime cycle, which thus leads to an appreciable positive radiative forcing (RF) (Bond et al., 2013); (ii) an indirect effect by forming contrails and contrail cirrus, which could be more significant than the direct effect (Bond et al., 2013). A recent study on the V2527-A5 engine of a research A320 airplane by Voigt et al. (Voigt et al., 2021) demonstrated that contrail ice particles (IP) are closely correlated to nvPM emissions and 80-90% of the IP have nvPM cores, indicating that such particles, although small in particle size (~ 20-30 nm), can serve as ice nucleus (IN) at the cruise condition (e.g. at T = 230 K and P = 25 kPa). From a recent study by Lee et al., the net effective RF induced by aviation activities is +100.9 mW/m^2 in 2018 mostly attributed to contrail cirrus (+57.4 mW/m^2) (Lee et al., 2021). It is generally agreed that the RF of contrail cirrus will increase in the coming years. This increase was estimated to occur by a factor of 3 from 2006 to 2050, reaching to 160 or even 180 mW/m^2 by then, attributed to both a large increase in air traffic and a slight shift in the air traffic towards high altitudes (Wilkerson et al., 2010; Bock and Burkhardt, 2019). According to the report by the Intergovernmental Panel on Climate Change (IPCC), RF from aviation could have a 7% contribution to anthropogenic RF by 2050 (Sabogal, 2011). A recent study provided experimental evidence that burning sustainable aviation fuels (SAF) can result in a 50 to 70% reduction of ice number concentration and a slight increase in ice crystal size

(Voigt et al., 2021). Although the formation and the evolution of contrails and contrail cirrus is one of the main undetermined factors that influence the prediction of future global radiation balance (Solomon et al., 2007), the microphysical interaction between aircraft nvPM emissions and the formation of contrails is still not fully understood.

Precise prediction of aviation nvPM emissions, especially those at cruise altitude, becomes critical in assessing the complex influences of aviation on climate. At present, there are several approaches being used to estimate the emission index for mass and number of nvPM (EI_m and EI_n), including the first order approximation version 3.0 (FOA3) (Wayson et al., 2009), the formation and oxidation (FOX) (Stettler et al., 2013a), the improved formation and oxidation (ImFOX) (Abrahamson et al., 2016), the approximation for soot from alternative fuels (ASAF) (Speth et al., 2015), and the smoke correlation for particle emission–CAEP11 (SCOPE11) (Agarwal et al., 2019). The FOA3 converts the results of smoke measurements, smoke numbers (SN), into nvPM mass concentrations. It was approved by ICAO (ICAO, 2011) in 2007 to evaluate nvPM emissions around airports worldwide. However, the SN instrument measures the light opacity of the particles collected on filter papers (ICAO, 2008). Its application to aviation emissions has been limited by two factors: insensitivity to ultrafine particles and insufficient resolution (Jones, 2002; Rye et al., 2012; Stettler et al., 2013b). Modern high-bypass turbofan aircraft engines such as the CFM56 and IAE-V2500 generate nvPM emissions in the range of 20-100 nm (Saffaripour et al., 2020; ICAO, 2021). For these engines, correlations between the nvPM mass concentrations and the SN are usually poor (Abrahamson et al., 2016). The FOX does not depend on SN measurement, but uses engine conditions as the input variables, thus avoiding the intrinsic uncertainties of SN measurement. However, the fuel parameters are not incorporated in the FOX model, so it may not be readily used to predict EI_m from SAFs, yet a study by Christie et al. showed that the FOA3 could still be valid for blends of SAFs with the conventional jet fuels (Christie et al., 2017). It has also been found that the predicted EI_m by FOX were about 4 times higher than the measurements (Abrahamson et al., 2016; Durdina et al., 2016; Durdina et al., 2017). In addition, Agarwal et al. developed a method for estimating EI_m and EI_n from aircraft engines, called SCOPE11 (Agarwal et al., 2019). This method predicts EI_n by assuming a log-normal size distribution and correlating geometric mean diameter (GMD) and geometric standard deviation (GSD) with a function of measured nvPM mass concentration. Similarly, because it is difficult to accurately measure the low SN produced by modern high bypass engines, the SCOPE11 is unreliable to predict nvPM emissions for low-emission engines.

SAF is one of the major and attractive solutions adopted by the global aviation community to mitigate aviation impact on climate (Undavalli and Khandelwal, 2021). A number of dedicated measurement programs have been carried out to evaluate the reduction of aviation emissions by using SAFs (Anderson et al., 2011; Beyersdorf et al., 2014; Moore et al., 2017; Durdina et al., 2021). For the purpose of estimating the effects of a variety of SAFs on nvPM emission mitigation, a new method called ASAF has been developed (Speth et al., 2015). The ASAF models the total rate of polycyclic aromatic hydrocarbons (soot precursor) formation as the sum of a component independent of fuel aromatic content and a component proportional to fuel aromatic content, and establishes the relationship between the total amount of nvPM generation and engine thrust setting, aromatic content of SAF and conventional aviation fuel. Through some assumptions and mathematical processing as well as combining with other estimation models suitable for conventional aviation fuel, the nvPM emissions burning SAFs can be predicted by the ASAF approach.

Most of the current predicting methods aim to estimate nvPM emissions around airports, which are important to local air quality and human health. However, in evaluating the influence of aviation on global radiative balance, emissions at cruise altitude contribute the most because the majority of the aviation fuel is consumed during cruise operation. A common approach to predict emissions at cruise altitude is to extrapolate the ground measurement values using dynamic ratios based on the Döpelheuer and Lecht correlation (Döpelheuer and Lecht, 1998). Abrahamson et al. developed the ImFOX, which can be directly used to predict nvPM emissions at cruise and burning SAFs (Abrahamson et al., 2016). However, the ImFOX only considers the hydrogen content of fuels and ignores the influence of other components, such as naphthalene and aromatics (Abrahamson et al., 2016), making the emission estimation values of the mode accurate for some specific data, but much less for other data, so the estimation values are still not satisfactory (Durdina et al., 2017). Previous studies showed that the content of naphthalene and aromatics in fuel can greatly affect aviation nvPM emissions (Moore et al., 2015; Durdina et al., 2017).

In recent years, artificial intelligent technologies such as machine learning methods have been applied broadly and successfully in various research areas (Ma et al., 2018; Nielsen and Voigt, 2018). As a representative of machine learning methods, neural network can obtain better fitting accuracy than the conventional linear statistical models by introducing nonlinear functions (Ukrainec et al., 1989). Until now, in the field of aviation emission estimation, there has been no attempt of using neural networks. Given that the prediction of aviation nvPM emissions is in fact a multiple regression problem, we believe that applying the convolutional neural network (CNN) approach in this field could provide a reasonable solution.

In this study, we develop a new approach based on CNN to estimate nvPM emissions from aircraft engines, by using a large variety of parameters about engine parameters, fuel properties, and ambient conditions as inputs. In particular, the newly published ICAO emission databank from ground tests and a series of open data from cruise experiments are utilized to develop the CNN model, which is capable of handling multi-dimensional data sets unlike the conventional empirical models. This study aims to address the following unsolved issues: (i) how to accurately predict emissions at cruise altitude based on emission measurements on the ground; (ii) how to estimate the impact of SAF under a wide range of engine conditions because there is limited experimental data using the SAF currently available. This approach can be used to improve nvPM inventory prediction from the current fleet and will be beneficial to evaluate the impact of aviation nvPM emissions on environment and climate change.

2. MATERIALS AND METHODS

In this study, we categorize five measurement data groups from four of previous aircraft field measurements either on the ground or at cruise altitude (Petzold et al., 1999; Schumann et al., 2002; Anderson et al., 2011; Moore et al., 2017; Voigt et al., 2021), and the ICAO 2021 Aircraft Engine Emissions Databank (EEDB) (ICAO, 2021). The comprehensive variables representing engine specific parameters (ESP), engine operational parameters (EOP), fuel properties (FP), and ambient conditions (AC) and nvPM emission data are used for the development of the predictive model of aviation nvPM emissions. We consider the influencing factors of nvPM emissions as the results of ESP, EOP, FP and AC, no matter whether the aircraft is on the ground or at cruise, burning conventional aviation fuels or SAFs. The input variables for the APMEP-CNN model in predicting EI_m and EI_n are the same and listed in the Table 1.

Table 1. Input Variables for the APMEP-CNN Model

Input Variables			
ESP	EOP	AC	FP
pressure ratio	fuel flow rate	ambient temperature	aromatics content
bypass ratio	thrust ratio	ambient pressure	
maximum rated thrust			

2.1. Measurement Data Sources

2.1.1. Emission Data for Aircrafts on the Ground

The EEDB provides the average values of nvPM emission measurement data for each engine with maximum rated thrust of more than 26.7 kN during the landing and take-off (LTO) cycle, which contains four specified thrust settings (ICAO, 2021). The EEDB includes the following information: (i) engine certification data, including bypass ratio, overall pressure ratio, and the maximum rated thrust under international standard atmospheric sea level static conditions (T = 288 K, P = 101325 Pa); (ii) fuel and combustion data, including the average heat of combustion of the fuel, hydrogen content, aromatics content, naphthalene content, sulfur content, and fuel flow rate; (iii) ambient data, including pressure, temperature, and relative humidity. In the EEDB, there are a total of 784 sets of measurement data for 196 engines from ten aircraft engine manufacturers. As shown is the EEDB, some of the reported EI_m and EI_n are corrected for system losses in accordance with the ICAO Appendix 8 of Annex 16 Vol II, but others are not.

2.1.2. Emission Data for Aircrafts at Cruise

Three of the five data groups used in the CNN modeling are the emission data of aircrafts at cruise from three field studies by Moore et al. (Moore et al., 2017), Voigt et al. (Voigt et al., 2021), and Schumann et al. (Petzold et al., 1999; Schumann et al., 2002), respectively. Moore et al. measured the emissions of the CFM56-2C1 engine equipped with the NASA DC-8 research aircraft from the NASA HU-25 Falcon aircraft using the NASA Langley Aerosol Research Group (LARGE) suite of in situ instruments, which were not corrected for diffusional, inertial and sedimentation losses given uncertainties associated with the condensation particle counter (CPC) detection efficiency curves (Moore et al., 2017). The uncertainty associated with neglecting these corrections was estimated to be 7%-9% on EI_n and around 3% on EI_m (Moore et al., 2017). They examined the influence of three different fuels, a low-sulfur-content Jet-A fuel, a medium-sulfur-content Jet-A fuel and a 50/50 (by volume) blend of the low-sulfur-content Jet-A fuel with an hydrotreated esters and fatty acids (HEFA) biojet fuel, on nvPM emissions at cruise (Moore et al., 2017). In the process of studying the influence of clean aviation fuels on the formation of contrail-induced clouds, Voigt et al. measured the emissions of the IAE-V2527-A5 engine equipped with an Airbus A320-232 aircraft with CPCs based on TSI, Model 3010 counters (TSI, Inc, USA), and provided the measured values of nvPM emissions under different fuel components, in which CPC data have been corrected for reduced detection efficiencies in low pressure environments and particle losses in the thermodenuder, with an overall uncertainty in nonvolatile particle number concentrations of ±15% (Voigt et al., 2021). Schumann et al. compiled the cruise data of aircraft nvPM emissions during the experiment of SULFUR 1-7, including the CF6-80C2A2, CFM56-3B1, CFM56-5C4 and PW JT3D-3B engines, and studied the influence of different sulfur contents on the composition of aircraft exhaust plumes (Petzold et al., 1999; Schumann et al., 2002). For these emission data, the loss correction was not mentioned in the paper.

2.1.3. Emission Data for Aircrafts burning Sustainable Aviation Fuels

The last data group is the compiled aircraft emission data based on the Alternative Aviation Fuel EXperiment I (AAFEX-I) field measurement campaign (Anderson et al., 2011), where five different fuels were tested: a standard JP-8 (or baseline) fuel and several commercially available SAFs, such as a Fischer-Tropsch (FT) fuel synthesized from natural gas (FT-1), a FT fuel prepared from coal (FT-2), and 50:50 blends of FT-1 and FT-2 with JP-8. The influence on the gaseous and PM emissions burning different fuels for CFM56-2C1 engines was systematically investigated by National Aeronautics and Space Administration (NASA) and collaborators. The CFM56 engine series are the most widely used engine type on commercial aircraft at present (almost all B737 use one version of this engine type). It should be noted that the AAFEX data sets are not corrected for the system line losses or background aerosol interference, different from the ICAO EEDB in the sampling, measurements and reporting practices since the ICAO EEDB complies with the Annex 16 requirements on nvPM emissions.

2.2. Modeling Procedure – the Convolutional Neural Network Method

The existing nvPM emission prediction models of aircraft engines are different in mechanism, characteristics and details, from the FOA3 which depends on SN and converts SN into nvPM mass concentrations, to the semi-empirical FOX and ImFOX which predict nvPM mass emissions based on the proprietary engine cycle data. In this study, we develop a new modeling method to predict nvPM emission indices for individual aircraft engine, based on the CNN technology. CNN is an end-to-end feature extraction method, of which two-dimensional (2D) convolution is suitable for image processing and one-dimensional (1D) convolution is usually used to deal with multiple regression problems. The detailed modelling procedure of the CNN approach used in this study is shown in Fig. 1.

There are four major steps during the CNN modeling procedure: data processing, model selection, model training and model prediction. In the first step, a process of feature selection is performed on the data relevant to nvPM emission. During the process, the Pearson correlation coefficient (PCC) and the maximum information coefficient (MIC) (Reshef et al., 2011) are used to select the attributing features that have a greater correlation with emission indices, to reduce modelling complexity, to improve the model capability and robustness, and to ensure the model accuracy. The selected features are the input variables for the APMEP-CNN model, which are listed in Table 1. After the feature selection, the EEDB data group with high-correlation characteristics are divided into three sets to train, validate and test the model. The training set, which uses approximately 60% of all the data, is to process the training error with the gradient descent method and learn the common parameters (such as weight coefficients, deviations, etc.) of the constructed regressor; the validation set, using 20% of all the data, is to adjust the hyperparameters of the regressor (such as the epochs, the number of network layers, the number of neurons in each layer, etc.) and preliminarily evaluate the capability of the model; and the test set, using the other 20% of all the data, is to measure the performance of the regressor and evaluate the generalization ability of the final model. About 60% of the other four data groups are used for testing as well, 20% and 20% are used for training and validation in order to make a correction to the data-driven model burning SAFs or at cruise.

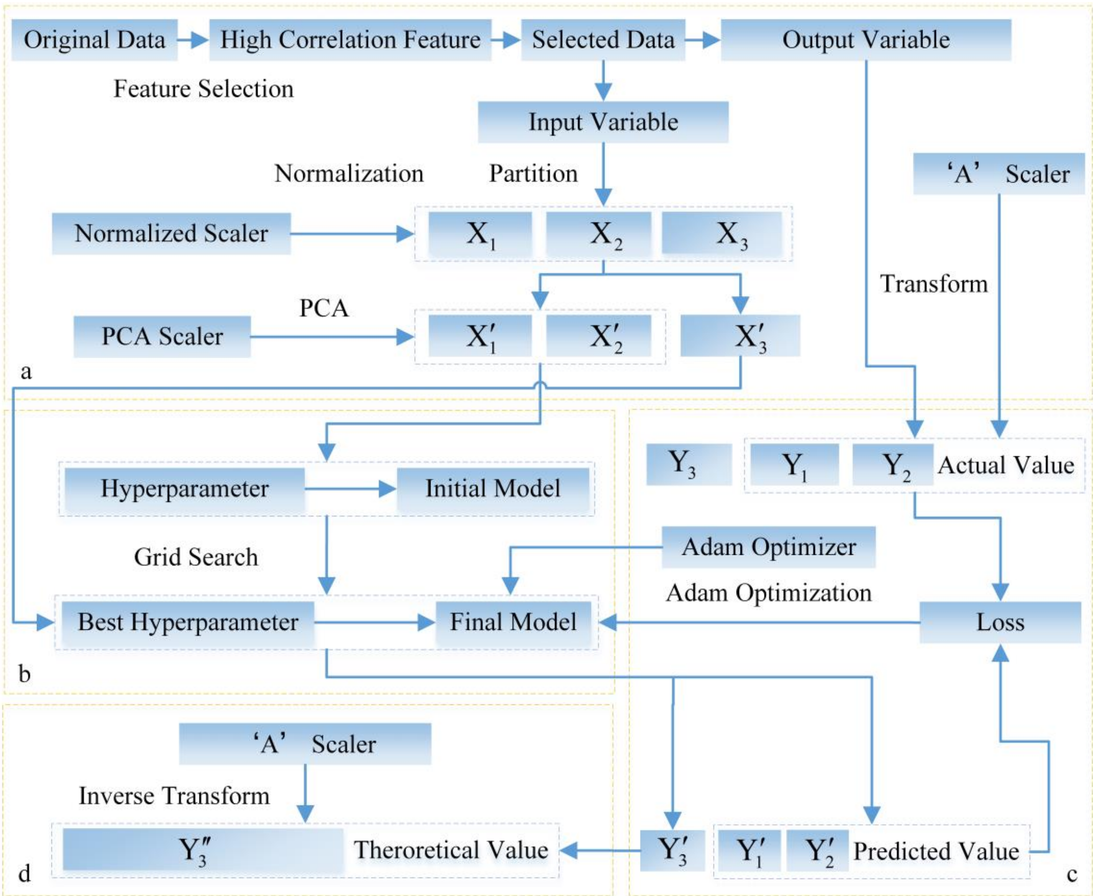

Figure 1. Establishment procedure of the proposed APMEP-CNN modelling approach. **a.** Data processing; **b.** Model selection; **c.** Model training; **d.** Model prediction. X_1, X_2, X_3 represent the normalized model training set, validation set and test set inputs. X_1', X_2', X_3' represent the input of model training set, validation set and test set after principal component analysis. Y_1, Y_2, Y_3 represent the experimental values of model training set, validation set and test set processed by 'A' scaler. Y_1', Y_2', Y_3' represent the output of model training set, validation set and test set in the iterative process. Y_3'' represent the output of model test set after inverse processing by 'A' scaler. 'A' scaler: logarithm the data before standardization.

All data are converted to be dimensionless by scaling to eliminate the problem of excessive differences among the used data, caused by the dimensional differences. The scaling process is beneficial to accelerate the convergence speed of model training and to improve the accuracy of the model. Among the data sets, the independent variables are normalized. To obtain better results in testing, EI_m and EI_n are converted to logarithms, and then the logarithm of EI_n is standardized. The goal of principal component analysis (PCA) is to map a high-dimensional data set into a low-dimensional space through certain linear projections, then to maximize the amount of data information (maximum variance) in the projected dimensions, leading to a reduction of data dimensions and still retaining original data characteristics. The dimensions after PCA for EI_m and EI_n are seven and eight, then the EI_m and EI_n are modeled as seven-dimensional and eight-dimensional structural models, respectively.

In the step of model selection, a hyperparametric data set is established by setting different numbers of hidden layers (1, 2), numbers of neurons (16, 32, 64, 128, 256, 512, 1024), epochs (500-5000 with a step of 50), and batch sizes (16, 32, 64, 128, 256, 512). A grid search experiment is then carried out on hyperparameters using K-fold cross-validation. Models with different hyperparameters are trained in the step of model training.

In this study, 1D convolution and max pooling operations are used to transform the high-dimensional data of the input layer to the hidden layer, extracting its features to reduce the dimensionality of the original data set effectively. The 1D convolution kernel and the pooling kernel slide along different experiment data to obtain features of ESP, EOP, FP and AC. As shown in Fig. 2 for EI_n, the experiment data have dimension N (N = 8). Blue boxes represent the convolution kernel with window length M (M = 3) and step length 1, and the feature dimension obtained by convolution is N - M + 1. Yellow boxes represent the pooling kernel with window length P (P = 2), and the feature dimension obtained by pooling is (N - M + 1) / P. Then, we have established a convolution-pooling module, and the feature mapping by convolution and pooling are shown in Eqs. 1 and 2 respectively.

$$v_j^l = f\left[\sum_{i \epsilon N} v_j^{l-1} k_{ij}^l + b_j^i\right] \tag{1}$$

where v_j^l is the convolution feature mapping of the j-th output of the neuron in layer l, v_j^{l-1} is the output of layer $l-1$, which is the input of layer l, k_{ij}^l is the coefficient in a convolution kernel from the i-th neuron in layer $l-1$ to the j-th neuron in layer l, b_j^i is the deviation of the j-th neuron in layer l, f is the Relu activation function (Glorot et al., 2011).

$$v_j^l = \max_{i^{l-1} \in N} v_j^{l-1} \tag{2}$$

where v_j^l is the pooling feature mapping of the j-th output of the neuron in layer l, v_j^{l-1} is the output of layer $l-1$, which is the input of layer l, $i^{l-1} \in N$ represents N output in layer $l-1$.

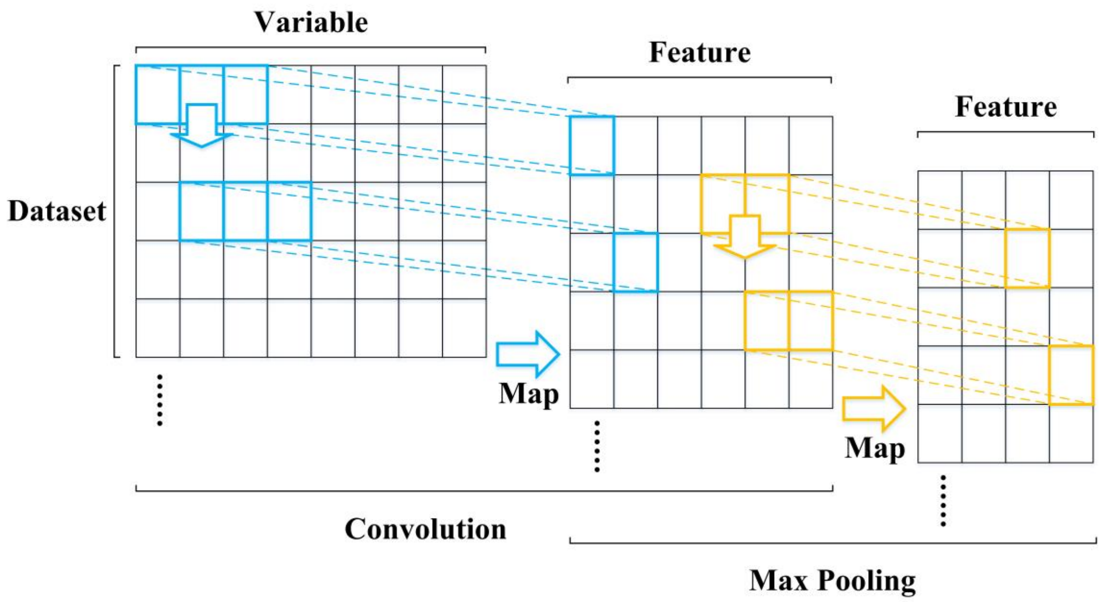

Figure 2. Operating principle of convolution kernel and pooling kernel. The blue and yellow boxes represent a convolution kernel with window length 3 and a pooling kernel with window length 2. The feature maps are obtained by sliding over the data related to engine emissions.

As shown in Fig. 3, the CNN constructed in this study for predicting EI_m is composed of two convolution layers with the window lengths of three and two, two max pooling layers with the window lengths of two and one, one flatten layer, one dropout layer and one fully connected layer. For EI_n, there are also two convolution layers with the window lengths of three and two, two max pooling layers with the window lengths of two and one. The pre-processed data is first extracted and dimensioned through the convolution layer and pooling layer, and then input to the flatten layer, which is used for the transition from the convolution layer to the fully connected layer to make the multi-dimensional data one-dimensional. The function of dropout layer is to randomly delete the neurons in the fully connected neural network with specified probability, to reduce the over-fitting effect and to enhance the robustness of the model. The last fully connected layer is used to synthesize the extracted features, which is described by the weight matrix of each neuron connection obtained by using the feedforward network topology with the back propagation (BP) algorithm.

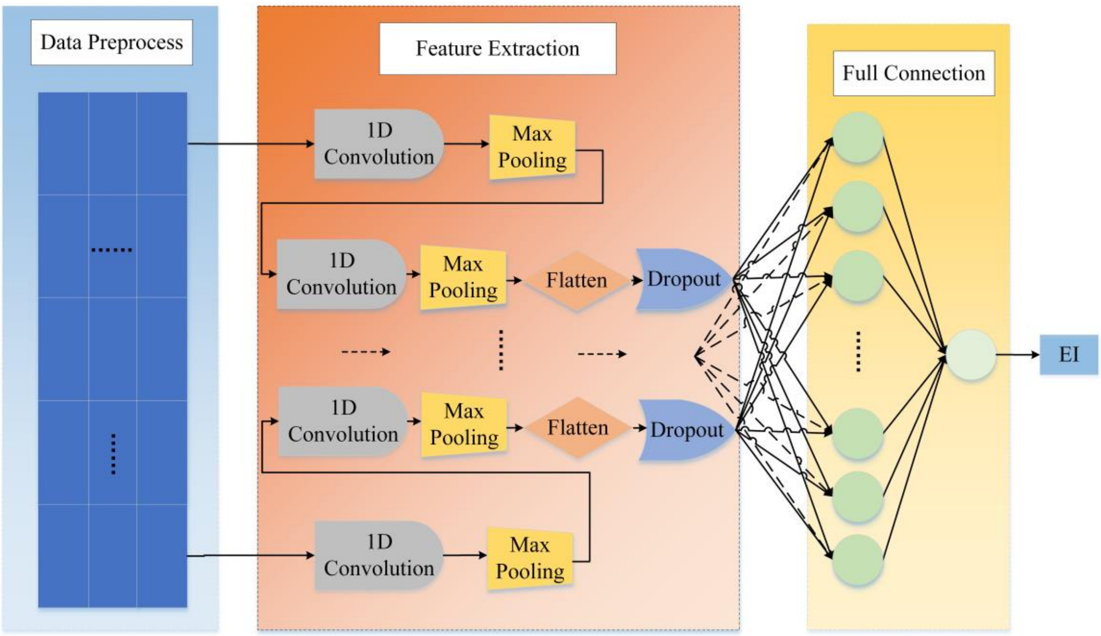

Figure 3. Network structure of the proposed APMEP-CNN model.

In the step of model training, the loss is calculated by taking the absolute value of the difference between the actual experimental value and the predicted value of the model, then put into the model to adjust the weights of all connections in the network, where, an adaptive optimization algorithm, called Adam, is used to be the optimizer (Kingma and Ba, 2014), with mean square error (MSE) as the loss function. This process continued until the set conditions are reached.

Finally, as the result of model selection, it is determined that the number of hidden layers is one and one; the number of neurons is 256 and 256; the epoch is 2840 and 3925; and the batch size is 128 and 256 for EI_m and EI_n respectively.

3. RESULTS AND DISCUSSION

3.1. Training/Validation and Test Results of the Convolutional Neural Network Method

In this study, the EEDB data group at ground level, namely take-off condition, climb-out condition, approach condition, idle condition, are divided into three sets, in which approximately 60% for training, 20% for validation, 20% for testing, while the other field measurement results are also divided into three sets, 20% for training, 20% for validation, and 60% for testing. The training/validation and the test results of EI_m and EI_n for 196 high-bypass turbofan aircraft engines predicted by the APMEP-CNN are shown in Fig. 4. There are 789 sets of data corrected and 51 sets of data uncorrected, thus the APMEP-CNN is a mixed model. To investigate the influence from the corrections for system losses, we establish three CNN models, labelled as model A, B, C, by using the fully corrected data, or the completely uncorrected data, or the mixed data, respectively. All the three models are used to calculate the nvPM emissions of five designated engines to evaluate the system error caused by the use of uncorrected data. The results (take RRMSE as the error index) are as follows: the EI_m calculated with model A differs from the experimental value by 0.161, the EI_n differs by 0.067; the EI_m calculated with model B differs by 0.237, the EI_n differs by 1.131; the EI_m calculated with model C differs by 0.300, and the EI_n differs by 0.098. Therefore, the EI_m system error caused by the use of the uncorrected data is 0.237, and the EI_n system error is 1.131.

The predicted training/validation and test values of EI_m and EI_n are in great agreement with the experimental data. As shown in Fig. 4b, 98.10% of the predicted EI_m are within a factor of two from the measured EI_m, compared to 48.3% for FOA3, 14.6% for FOX and 24.7% for ImFOX. Similarly, 99.37% of the predicted EI_n are within a factor of two from the measured EI_n in Fig. 4d. From a consequent correlation analysis, the test results are satisfactory with the relative root mean square error

(RRMSE, dividing the root mean square error by the average of the measurement values) being 0.34, 0.23, and the coefficient of determination (R^2) being 0.96, 0.96 for EI_m and EI_n respectively. It should be noted that the plots in Fig. 4 are in log-log scale, so majority of the agreements between the APMEP-CNN model and experimental measurements seen in the plots are within a factor of less than 2.

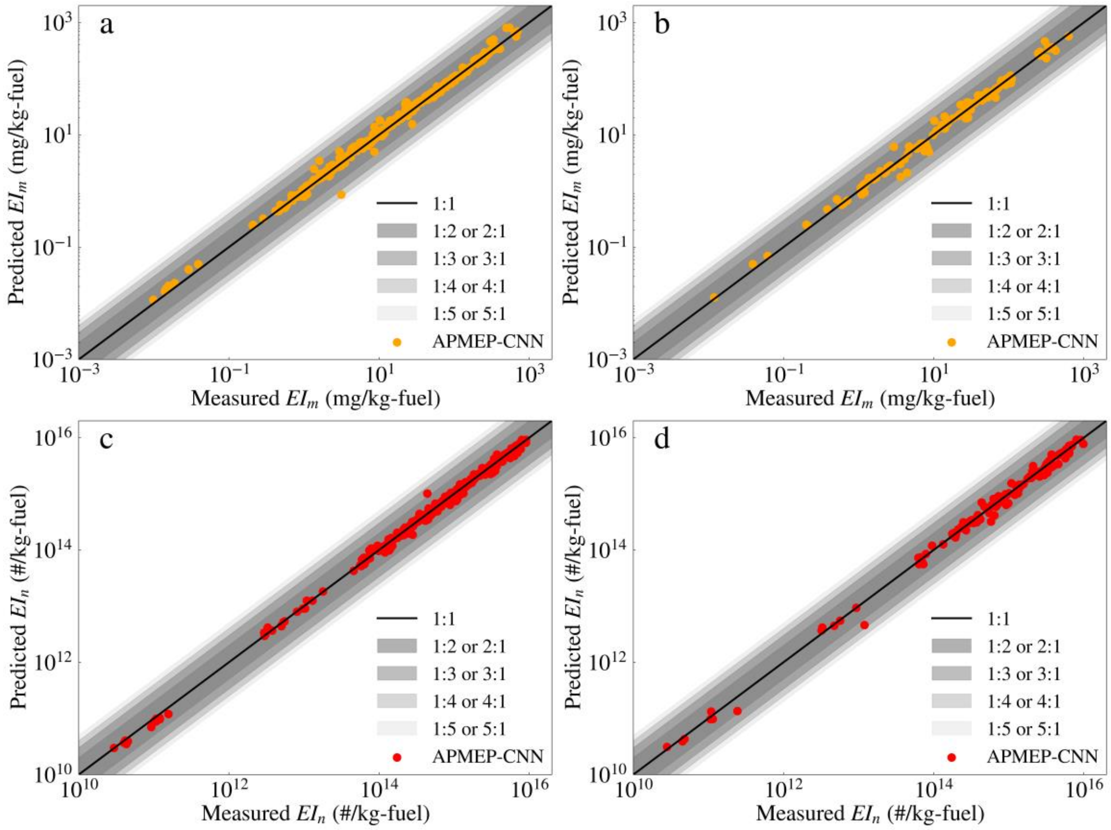

Figure 4. Comparison between the predicted and measured emission indices using the APMEP-CNN for the training/validation and test data sets. **a.** Results of EI_m from the training (60%) and validation (20%) data set; **b.** Results of EI_m from the test (20%) data set; **c.** Results of EI_n from the training (60%) and validation (20%) data set; **d.** Results of EI_n from the test (20%) data set. Shaded gray areas with different transparency

represent error bounds with different sizes.

3.2. Predictions of nvPM Emissions during the LTO Cycle

In order to evaluate the predictive accuracy of the APMEP-CNN compared with other existing models, measurement data in the EEDB related to 76 aircraft engines for APMEP-CNN, FOX and ImFOX, and 74 for FOA3, are utilized to predict nvPM emissions during the LTO cycle (These measurement data haven't been used in the training or validation step, but only for testing. The data in Section 3.3 and 3.4 is the same). In Fig. 5, a comparison between predicted and measured values of EI_m at the ICAO certification test points (i.e., 7, 30, 85, 100% thrust) using four models is shown in a log-log scale.

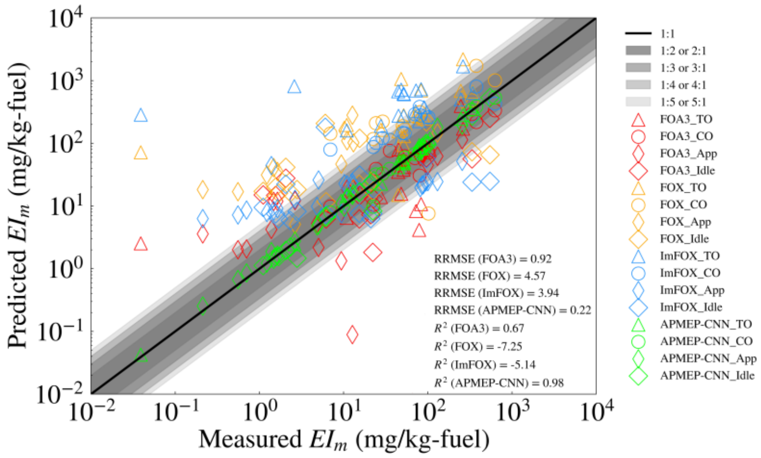

Figure 5. Comparison between predicted EI_m using different models with measured EI_m in the ICAO EEDB. Shaded gray areas with different transparency represent error bounds with different sizes.

The prediction of the APMEP-CNN correlates better with the measurements than those of FOA3, FOX and ImFOX, with RRMSE = 0.22, R^2 = 0.98 for APMEP-CNN; RRMSE = 0.92, R^2 = 0.67 for FOA3; $R^2 < 0$ for FOX and ImFOX. When using the FOX to estimate EI_m, about 17.1% of the total results are negative. For the current version of FOX and ImFOX, the predicted EI_m are overestimated especially at take-off and climb-out, as displayed in Fig. 5. The negative R^2 values indicates that FOX and ImFOX perform worse than a mean EI_m value, suggesting that these two methods might be unsuitable for newer high-bypass gas turbine engines in the EEDB. However, the FOX and the ImFOX are promising in describing the clear trend between EI_m and thrust, also they are suitable for predicting nvPM emissions from older engines (Stettler et al., 2013a; Abrahamson et al., 2016). As shown in Fig. 5, the majority of EI_m predicted by FOA3 are lower than the measured values. There may be three reasons for the underestimation from FOA3: (i) the insufficient resolution in measuring SN at low emissions, since the prediction of the FOA3 is based on the SN measurements of aircraft engines, which tend to underestimate when the emissions are low (Stettler et al., 2013b); (ii) the insensitivity in detecting small particles as nvPM from turbofan aircraft engines is normally in the range of 20-100 nm (Saffaripour et al., 2020); and (iii) the difference in the SN measurements by engine manufacturers. However, the FOA3 is still highly valuable because it can be applied universally across all combustor technologies as long as SN can be accurately measured (Abrahamson et al., 2016). For four thrust settings, 97.4% of the APMEP-CNN predictions agree to within a factor of two from the measurements, representing an improvement compared with other methods.

3.3. Predictions of nvPM Emissions at Cruise

Because the training and validation processes have used the measurement results at both the ground level and cruise, the APMEP-CNN can also be used to predict nvPM emissions during cruise operations. Our prediction are compared with previous measurement studies on six commercial aircraft engines, including CF6-80C2A2, CFM56-3B1, CFM56-5C4, JT3D-3B, CFM56-2C1, and V2527-A5 during the SULFUR 1-7 experiments, the ACCESS experiments and the ECLIF projects (Petzold et al., 1999; Schumann et al., 2002; Moore et al., 2017; Voigt et al., 2021). The predicted values and the measurement values are listed in Table 2, in which the predicted EI_m of the CF6-80C2A2, CFM56-3B1, CFM56-5C4, JT3D-3B, CFM56-2C1 and V2527-A5 engines are different from the measurements (Petzold et al., 1999; Schumann et al., 2002; Moore et al., 2017; Voigt et al., 2021) by 21.1%, 27.3%, 60.0%, -69.2%, 4.5% and * respectively (* means there is no measurement data), while for the predicted EI_n, the differences are 38.8%, 44.3%, 53.3%, -24.8%, 36.5% and 46.6%, respectively.

Conventionally, both the FOA3 and the FOX predict engine emissions during cruise operation by using the dynamic ratio relationship proposed by Döpelheuer and Lecht to scale the ground values to the cruise values (Döpelheuer and Lecht, 1998; Stettler et al., 2013a). When the ICAO-certified SN results are used to estimate nvPM emissions at cruise, the predicted values of EI_m are usually smaller than the measurement results. Some previous studies have shown that the updated FOA3 could also lead to an underestimation(Stettler et al., 2013a; Abrahamson et al., 2016).. The ImFOX uses a direct cruise prediction method (Abrahamson et al., 2016), which only needs the information for fuel flow rate and fuel hydrogen content as the inputs to calculate the EI_m at cruise. However, we find that the ImFOX predictions of EI_m are quite different from the measurement results. In terms of parameter selection, the APMEP-CNN model is quite different from the conventional models, capable of considering more relevant parameters as the input parameters, thus can provide better predictions than the conventional models.

Table 2. Comparison between Measured and Predicted Emission Indices at Cruise

Aircraft	A310-300	B737-300	A340	B707	DC-8	A320
Engine	CF6-80C2A2	CFM56-3B1	CFM56-5C4	JT3D-3B	CFM56-2C1	V2527-A5
Power (%)	18.9	22.5	19.9	40.0	24.8	29.9
EI_m_measured [a]	19 ± 10	11 ± 5	10 ± 3	500 ± 100	22 [c]	\

EI_n_measured [b]	6 ± 1.2	3.5 ± 0.7	1.8 ± 0.5	17 ± 3	4.99 [c]	27
EI_m_APMEP-CNN [a]	23 [d]	14 [d]	16 [d]	154 [d]	23 [c]	48
EI_n_APMEP-CNN [b]	8.33 [d]	5.05 [d]	2.76 [d]	12.78 [d]	6.81 [c]	39.58

[a] In the unit of mg/kg-fuel; [b] In the unit of 10^{14} #/kg-fuel; [c] Not corrected for system losses; [d] There are no data for the aromatics content in these measurements, thus we establish a model using hydrogen content as one of the CNN input variables, instead of aromatic content; \ No measurement data.

3.4. Predictions of nvPM Emissions burning Sustainable Aviation Fuels

Because the training and validation processes have used the measurement results from aircraft engines burning both conventional aviation fuels or SAFs, the APMEP-CNN can also be used to predict nvPM emissions burning different fuels. The predicted EI_m of the CFM56-2C1 engine burning JP-8, FT-1, FT-2, the mixed fuel Blend-1 and Blend-2 under different engine thrusts are shown in Fig. 6, in comparison with the measured results. The APMEP-CNN can predict the values of EI_m with RRMSE = 0.48, R^2 = 0.89, and EI_n with RRMSE = 0.27, R^2 = 0.91.

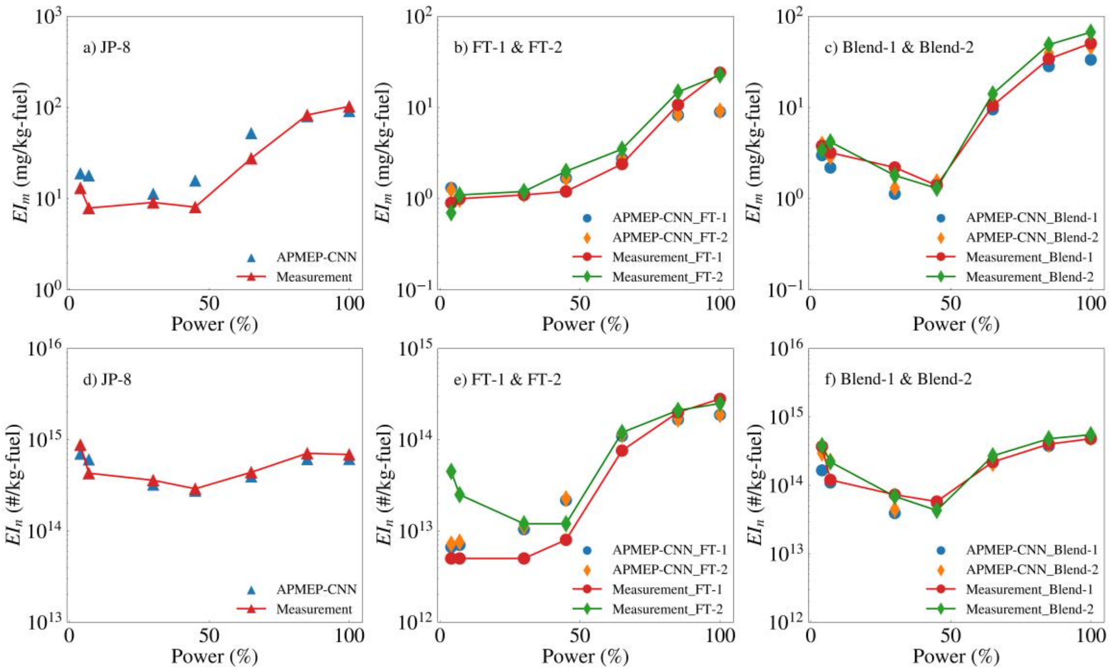

Figure 6. Comparison between the predicted emission indices of nvPM using the APMEP-CNN model with the measured results for the CFM56-2C1 engine while burning JP-8, FT-1, FT-2, Blend-1 and Blend-2 during the AAFEX-I campaign. **a)** The EI_m burning JP-8 vs engine power; **b)** The EI_m burning FT-1 and FT-2 vs engine power; **c)** The EI_m burning Blend-1 and Blend-2 vs engine power; **d)** The EI_n burning JP-8 vs engine power; **e)** The EI_n burning FT-1 and FT-2 vs engine power; **f)** The EI_n burning Blend-1 and Blend-2 vs engine power.

As displayed in six subgraphs of Fig. 6, the APMEP-CNN is able to capture the relationship between the nvPM emissions and the variation in fuel composition, in which the increase of aromatic and naphthalene content or the decrease of hydrogen content results in the increase of EI_m and EI_n, as observed by previous studies (Marx and Namer, 1988; Corporan et al., 2004; Corporan et al., 2007; DeWitt et al., 2008; Timko et al., 2010; Corporan et al., 2011; Cain et al., 2013; Beyersdorf et al., 2014; Brem et al., 2015; Durand et al., 2021). The reason for the predictive accuracy of the APMEP-CNN model maybe twofold: (i) the APMEP-CNN considers both fuel components and engine optional parameters,; (ii) the APMEP-CNN uses the most recent emission measurements of EI_m and EI_n from the ICAO EEDB (ICAO, 2021). This also confirms the important influence of fuel properties on aviation nvPM formation (Moore et al., 2015).

4. CONCLUSIONS

In conclusion, with the newly published ICAO emission databank and extra open measurement results from several field campaigns including cruise tests and SAF tests, we develop the APMEP-CNN, a new aviation nvPM emission predictive model via convolutional neural network, which can predict nvPM emissions on the ground and at cruise for a large number of high-bypass commercial aircraft turbofan engines burning either conventional aviation fuels or SAFs. The developed APMEP-CNN model has been demonstrated to be able to provide relatively accurate estimates of nvPM emissions. Further measurements of aviation emissions during cruise operation will be helpful to further verify the APMEP-CNN and eventually enable establishment of a more accurate global inventory of aviation nvPM emissions.

In despite of the success in predicting aviation nvPM emissions, the APMEP-CNN still has two intrinsic limitations: (i) the complexity of such brain-inspired neural networks makes them remarkably capable, yet it also renders them opaque to human understanding, turning them into ‘black-box’ systems, which means that researchers cannot trace the course of the neural network calculations. However, we demonstrated that the satisfactory estimation of nvPM emissions can be achieved with a certain degree of accuracy; (ii) compared with traditional aviation nvPM emission prediction methods, the APMEP-CNN usually needs a large quantity of measurement data. Although this approach makes a reasonable prediction of nvPM emissions, the amount of training data could be still insufficient, and the acquisition of a large number of relevant data is a major challenge in the field of aviation emission, especially at cruise. Alternatively, a flight simulation ground test facility, which can simulate flight conditions by providing airflow at pressures and temperatures experienced at cruise, may be used to alleviate the scarcity of cruise data by conducting cruise-like experiments with dramatically lower costs and higher accuracy. In the future, with the continuous progress of relevant measurements both on the ground and at cruise (or cruise simulation ground tests) burning both conventional aviation fuels and SAFs, the APMEP-CNN may achieve even more accurate prediction results. To address the opaqueness issue of mainstream neural networks, some new and promising transparent machine learning techniques could be utilized, which could offer system transparency to enable us to form coherent explanations of the system's decisions and actions without sacrificing prediction accuracy.

NOMENCLATURE

Abbreviation	Full Name
AAFEX-I	Alternative Aviation Fuel EXperiment I
AC	Ambient Condition
ACCESS	Alternative Fuel Effects on Contrails and Cruise Emissions Study
APMEP-CNN	Aviation nvPM Emission Prediction Based on the Convolutional Neural Network
ASAF	Approximation for Soot from Alternative Fuels
BC	Black Carbon
BP	Back Propagation

CNN	Convolutional Neural Network
CPC	Condensation Particle Counter
EEDB	Engine Emissions Database
EI_m	Mass Emission Index
EI_n	Number Emission Index
EOP	Engine Operational Parameter
ESP	Engine Specific Parameter
FOA3	First Order Approximation Version 3.0
FOX	Formation and Oxidation
FP	Fuel Property
FT	Fischer-Tropsch
GMD	Geometric Mean Diameter
GSD	Geometric Standard Deviation
HEFA	Hydrotreated Esters and Fatty Acids
ICAO	International Civil Aviation Organization
ImFOX	Improved Formation and Oxidation
IN	Ice Nucleus
IP	Ice Particle

IPCC	Intergovernmental Panel on Climate Change
LARGE	Langley Aerosol Research Group
LTO	Landing and Take-off
MIC	Maximum Information Coefficient
MSE	Mean Square Error
NASA	National Aeronautics and Space Administration
nvPM	Non-volatile Particulate Matter
PCA	Principal Component Analysis
PCC	Pearson Correlation Coefficient
R^2	the Coefficient of Determination
RF	Radiative Forcing
RRMSE	Relative Root Mean Square Error
SAF	Sustainable Aviation Fuel
SCOPE11	Smoke Correlation for Particle Emission–CAEP11
SN	Smoke Number
1D	One-Dimensional
2D	Two-Dimensional

DECLARATION OF COMPETING INTEREST

The authors declare that they have no known competing financial interests or personal relationships that could have appeared to influence the work reported in this paper.

ACKNOWLEDGMENTS

This work was mainly supported by the National Natural Science Foundation of China (51922019 & 51920105009). This work was also partially supported by National Engineering Laboratory for Mobile Source Emission Control Technology (NELMS2018A02), Open Foundation of Beijing Key Laboratory of Occupational Safety and Health (2019) and the Reform and Development Project of Beijing Municipal Institute of Labour Protection (2020).

REFERENCES

Abrahamson, J.P., Zelina, J., Andac, M.G., Vander Wal, R.L., 2016. Predictive Model Development for Aviation Black Carbon Mass Emissions from Alternative and Conventional Fuels at Ground and Cruise. Environ. Sci. Technol. 50(21), 12048-12055. http://dx.doi.org/10.1021/acs.est.6b03749.

Agarwal, A., Speth, R.L., Fritz, T.M., Jacob, S.D., Rindlisbacher, T., Iovinelli, R., Owen, B., Miake-Lye, R.C., Sabnis, J.S., Barrett, S.R.H., 2019. SCOPE11 Method for Estimating Aircraft Black Carbon Mass and Particle Number Emissions. Environ. Sci. Technol. 53(3), 1364-1373. http://dx.doi.org/10.1021/acs.est.8b04060.

Anderson, B. E., Beyersdorf, A.J., Hudgins, C.H., Plant, J.V., Thornhill, K.L., Winstead, E.L., 2011. Alternative aviation fuel experiment (AAFEX). National Aeronautics and Space Administration, Langley Research Center, Hampton, VA.

Beyersdorf, A.J., Timko, M.T., Ziemba, L.D., Bulzan, D., Corporan, E., Herndon, S.C., Howard, R., Miake-Lye, R., Thornhill, K.L., Winstead, E., Wey, C., Yu, Z., Anderson, B.E., 2014. Reductions in aircraft particulate emissions due to the use of Fischer-Tropsch fuels. Atmos. Chem. Phys. 14(1), 11-23. http://dx.doi.org/10.5194/acp-14-11-2014.

Bock, L., Burkhardt, U., 2019. Contrail cirrus radiative forcing for future air traffic. Atmos. Chem. Phys. 19(12), 8163-8174. http://dx.doi.org/10.5194/acp-19-8163-2019.

Bond, T.C., Doherty, S.J., Fahey, D.W., Forster, P.M., Berntsen, T., DeAngelo, B.J., Flanner, M.G., Ghan, S., Karcher, B., Koch, D., Kinne, S., Kondo, Y., Quinn, P.K., Sarofim, M.C., Schultz, M.G., Schulz, M., Venkataraman, C., Zhang, H., Zhang, S., Bellouin, N., Guttikunda, S.K., Hopke, P.K., Jacobson, M.Z., Kaiser, J.W., Klimont, Z., Lohmann, U., Schwarz, J.P., Shindell, D., Storelvmo, T., Warren, S.G., Zender, C.S., 2013. Bounding the role of black carbon in the climate system: A scientific assessment. J. Geophys. Res.-Atmos. 118(11), 5380-5552. http://dx.doi.org/10.1002/jgrd.50171.

Brem, B.T., Durdina, L., Siegeris, F., Beyerle, P., Bruderer, K., Rindlisbacher, T., Rocci-Denis, S., Andac, M.G., Zelina, J., Penanhoat, O., Wang, J., 2015. Effects of Fuel Aromatic Content on Nonvolatile Particulate Emissions of an In-Production Aircraft Gas Turbine. Environ. Sci. Technol. 49(22), 13149-13157. http://dx.doi.org/10.1021/acs.est.5b04167.

Cain, J., DeWitt, M.J., Blunck, D., Corporan, E., Striebich, R., Anneken, D., Klingshirn, C., Roquemore, W.M., Vander Wal, R., 2013. Characterization of Gaseous and Particulate Emissions From a Turboshaft Engine Burning Conventional, Alternative, and Surrogate Fuels. Energ. Fuel. 27(4), 2290-2302. http://dx.doi.org/10.1021/ef400009c.

Christie, S., Lobo, P., Lee, D., Raper, D., 2017. Gas Turbine Engine Nonvolatile Particulate Matter Mass Emissions: Correlation with Smoke Number for Conventional and Alternative Fuel Blends. Environ. Sci. Technol. 51(2), 988-996. http://dx.doi.org/10.1021/acs.est.6b03766.

Corporan, E., DeWitt, M., Wagner, M., 2004. Evaluation of soot particulate mitigation additives in a T63 engine. Fuel Process. Technol. 85(6-7), 727-742. http://dx.doi.org/10.1016/j.fuproc.2003.11.016.

Corporan, E., DeWitt, M.J., Belovich, V., Pawlik, R., Lynch, A.C., Gord, J.R., Meyer, T.R., 2007. Emissions characteristics of a turbine engine and research combustor burning a Fischer-Tropsch jet fuel. Energ. Fuel. 21(5), 2615-2626. http://dx.doi.org/10.1021/ef070015j.

Corporan, E., Edwards, T., Shafer, L., DeWitt, M.J., Klingshirn, C., Zabarnick, S., West, Z., Striebich, R., Graham, J., Klein, J., 2011. Chemical, Thermal Stability, Seal Swell, and Emissions Studies of Alternative Jet Fuels. Energ. Fuel. 25(3), 955-966. http://dx.doi.org/10.1021/ef101520v.

DeWitt, M.J., Corporan, E., Graham, J., Minus, D., 2008. Effects of Aromatic Type and Concentration in Fischer−Tropsch Fuel on Emissions Production and Material Compatibility. Energ. Fuel. 22(4), 2411-2418. http://dx.doi.org/10.1021/ef8001179.

Döpelheuer, A., Lecht, M., 1998. Influence of engine performance on emission characteristics, RTO/AVT Symposium on "Gas Turbine Combustion, Emissions and Alternative Fuels", Lisboa, Portugal p. RTO MP-14.

Durand, E., Lobo, P., Crayford, A., Sevcenco, Y., Christie, S., 2021. Impact of fuel hydrogen content on non-volatile particulate matter emitted from an aircraft auxiliary power unit measured with standardised reference systems. Fuel. 287, 119637. http://dx.doi.org/10.1016/j.fuel.2020.119637.

Durdina, L., Brem, B.T., Elser, M., Schonenberger, D., Siegerist, F., Anet, J.G., 2021. Reduction of Nonvolatile Particulate Matter Emissions of a Commercial Turbofan Engine at the Ground Level from the Use of a Sustainable Aviation Fuel Blend. Environ. Sci. Technol. 55(21), 14576-14585.

http://dx.doi.org/10.1021/acs.est.1c04744.

Durdina, L., Brem, B.T., Setyan, A., Siegeris, F., Rindlisbacher, T., Jing, W., 2017. Assessment of Particle Pollution from Jetliners: from Smoke Visibility to Nanoparticle Counting. Environ. Sci. Technol. 51(6), 3534-3541. http://dx.doi.org/10.1021/acs.est.6b05801.

Durdina, L., Brem, B.T., Wang, J., 2016. Implications of the New PM Emission Standard for Jet Engines, 20th ETH Conference on Combustion Generated Nanoparticles, ETH Zurich, Switzerland.

Glorot, X., Bordes, A., Bengio, Y., 2011. Deep Sparse Rectifier Neural Networks. PMLR: 15, 315-323.

ICAO, 2008. ICAO Annex 16: Environmental Protection, Vol. II – Aircraft Engine Emissions. International Civil Aviation Organization, Montreal, Canada.

ICAO, 2011. Airport Air QualityManual. International Civil Aviation Organization, Montreal, Canada.

ICAO, 2021. EASA ICAO Engine Emissions Databank. The European Union Aviation Safety Agency.

Jensen, E.J., Toon, O.B., 1997. The potential impact of soot particles from aircraft exhaust on cirrus clouds. Geophys. Res. Lett. 24(3), 249-252. http://dx.doi.org/10.1029/96gl03235.

Jones, M., 2002. Advanced Opacity Meters: Their Potential Role in Future Emission Testing Legislation for Diesel Vehicles, Proc. of the 6th ETH Conference on Nanoparticle Measurement, Zurich.

Kingma, D., Ba, J., 2014. Adam: A Method for Stochastic Optimization. Computer Science. http://dx.doi.org/10.48550/arXiv.1412.6980.

Lee, D.S., Fahey, D.W., Forster, P.M., Newton, P.J., Wit, R.C.N., Lim, L.L., Owen, B., Sausen, R., 2009.

Aviation and global climate change in the 21st century. Atmospheric Environ. 43(22-23), 3520-3537. http://dx.doi.org/10.1016/j.atmosenv.2009.04.024.

Lee, D.S., Fahey, D.W., Skowron, A., Allen, M.R., Burkhardt, U., Chen, Q., Doherty, S.J., Freeman, S., Forster, P.M., Fuglestvedt, J., Gettelman, A., De Leon, R.R., Lim, L.L., Lund, M.T., Millar, R.J., Owen, B., Penner, J.E., Pitari, G., Prather, M.J., Sausen, R., Wilcox, L.J., 2021. The contribution of global aviation to anthropogenic climate forcing for 2000 to 2018. Atmospheric Environ. 244, 117834. http://dx.doi.org/10.1016/j.atmosenv.2020.117834.

Liati, A., Brem, B.T., Durdina, L., Vogtli, M., Dasilva, Y.A.R., Eggenschwiler, P.D., Wang, J., 2014. Electron Microscopic Study of Soot Particulate Matter Emissions from Aircraft Turbine Engines. Environ. Sci. Technol. 48(18), 10975-10983. http://dx.doi.org/10.1021/es501809b.

Lobo, P., Condevaux, J., Yu, Z.H., Kuhlmann, J., Hagen, D.E., Miake-Lye, R.C., Whitefield, P.D., Raper, D.W., 2016. Demonstration of a Regulatory Method for Aircraft Engine Nonvolatile PM Emissions Measurements with Conventional and Isoparaffinic Kerosene fuels. Energ. Fuel. 30(9), 7770-7777. http://dx.doi.org/10.1021/acs.energyfuels.6b01581.

Lobo, P., Durdina, L., Smallwood, G.J., Rindlisbacher, T., Siegerist, F., Black, E.A., Yu, Z.H., Mensah, A.A., Hagen, D.E., Miake-Lye, R.C., Thomson, K.A., Brem, B.T., Corbin, J.C., Abegglen, M., Sierau, B., Whitefield, P.D., Wang, J., 2015. Measurement of Aircraft Engine Non-Volatile PM Emissions: Results of the Aviation-Particle Regulatory Instrumentation Demonstration Experiment (A-PRIDE)

4 Campaign. Aerosol Sci. Tech. 49(7), 472-484. http://dx.doi.org/10.1080/02786826.2015.1047012.

Ma, J.Z., Yu, M.K., Fong, S., Ono, K., Sage, E., Demchak, B., Sharan, R., Ideker, T., 2018. Using deep learning to model the hierarchical structure and function of a cell. Nat. Methods. 15(4), 290-298. http://dx.doi.org/10.1038/Nmeth.4627.

Marx, M.M., Namer, I., 1988. A gas turbine emissions model as a function of engine operating conditions, fuel properties, and combustor geometry, 26th Aerospace Sciences Meeting, Reno, Nevada; American Institute of Aeronatics and Astronautics: Reston, VA, USA. https://doi.org/10.2514/6.1988-153

Moore, R.H., Shook, M., Beyersdorf, A., Corr, C., Herndon, S., Knighton, W.B., Miake-Lye, R., Thornhill, K.L., Winstead, E.L., Yu, Z.H., Ziemba, L.D., Anderson, B.E., 2015. Influence of Jet Fuel Composition on Aircraft Engine Emissions: A Synthesis of Aerosol Emissions Data from the NASA APEX, AAFEX, and ACCESS Missions. Energ. Fuel. 29(4), 2591-2600. http://dx.doi.org/10.1021/ef502618w.

Moore, R.H., Thornhill, K.L., Weinzierl, B., Sauer, D., D'Ascoli, E., Kim, J., Lichtenstern, M., Scheibe, M., Beaton, B., Beyersdorf, A.J., Barrick, J., Bulzan, D., Corr, C.A., Crosbie, E., Jurkat, T., Martin, R., Riddick, D., Shook, M., Slover, G., Voigt, C., White, R., Winstead, E., Yasky, R., Ziemba, L.D., Brown, A., Schlager, H., Anderson, B.E., 2017. Biofuel blending reduces particle emissions from aircraft engines at cruise conditions. Nature. 543(7645), 411-415.

http://dx.doi.org/10.1038/nature21420.

Nielsen, A.A.K., Voigt, C.A., 2018. Deep learning to predict the lab-of-origin of engineered DNA. Nat. Commun. 9(1), 3135. http://dx.doi.org/10.1038/s41467-018-05378-z.

Peck, J., Oluwole, O.O., Wong, H.W., Miake-Lye, R.C., 2013. An algorithm to estimate aircraft cruise black carbon emissions for use in developing a cruise emissions inventory. J. Air Waste Manage. 63(3), 367-375. http://dx.doi.org/10.1080/10962247.2012.751467.

Petzold, A., Dopelheuer, A., Brock, C.A., Schroder, F., 1999. In situ observations and model calculations of black carbon emission by aircraft at cruise altitude. J. Geophys. Res.-Atmos. 104(D18), 22171-22181. http://dx.doi.org/10.1029/1999jd900460.

Reshef, D.N., Reshef, Y.A., Finucane, H.K., Grossman, S.R., McVean, G., Turnbaugh, P.J., Lander, E.S., Mitzenmacher, M., Sabeti, P.C., 2011. Detecting Novel Associations in Large Data Sets. Science. 334(6062), 1518-1524. http://dx.doi.org/10.1126/science.1205438.

Rye, L., Lobo, P., Williams, P.I., Uryga-Bugajska, I., Christie, S., Wilson, C., Hagen, D., Whitefield, P., Blakey, S., Coe, H., Raper, D., Pourkashanian, M., 2012. Inadequacy of Optical Smoke Measurements for Characterization of Non-Light Absorbing Particulate Matter Emissions from Gas Turbine Engines. Combust. Sci. Technol. 184(12), 2068-2083. http://dx.doi.org/10.1080/00102202.2012.697499.

Sabogal, N., 2011. A Brief Summary of the Special Report on Aviation and the Global Atmosphere.

Perspectiva Geográfica. 1(5), 74-76.

Saffaripour, M., Thomson, K.A., Smallwood, G.J., Lobo, P., 2020. A review on the morphological properties of non-volatile particulate matter emissions from aircraft turbine engines. J. Aerosol Sci. 139, 105467. http://dx.doi.org/10.1016/j.jaerosci.2019.105467.

Schumann, U., Arnold, F., Busen, R., Curtius, J., Karcher, B., Kiendler, A., Petzold, A., Schlager, H., Schroder, F., Wohlfrom, K.H., 2002. Influence of fuel sulfur on the composition of aircraft exhaust plumes: The experiments SULFUR 1-7. J. Geophys. Res.-Atmos. 107(D15), 4247. http://dx.doi.org/10.1029/2001jd000813.

Solomon, S.D., Qin, D., Manning, M., Chen, Z., Miller, H.L., 2007. Climate Change 2007 : the physical science basis. Working Group I contribution to the fourth assessment report of the IPCC. intergovernmental panel on climate change climate change. http://dx.doi.org/10.1016/S0925-7721(01)00003-7.

Speth, R.L., Rojo, C., Malina, R., Barrett, S.R.H., 2015. Black carbon emissions reductions from combustion of alternative jet fuels. Atmospheric Environ. 105, 37-42. http://dx.doi.org/10.1016/j.atmosenv.2015.01.040.

Stettler, M.E.J., Boies, A.M., Petzold, A., Barrett, S.R.H., 2013a. Global Civil Aviation Black Carbon Emissions. Environ. Sci. Technol. 47(18), 10397-10404. http://dx.doi.org/10.1021/es401356v.

Stettler, M.E.J., Eastham, S., Barrett, S.R.H., 2011. Air quality and public health impacts of UK airports.

Part I: Emissions. Atmospheric Environ. 45(31), 5415-5424. http://dx.doi.org/10.1016/j.atmosenv.2011.07.012.

Stettler, M.E.J., Swanson, J.J., Barrett, S.R.H., Boies, A.M., 2013b. Updated Correlation Between Aircraft Smoke Number and Black Carbon Concentration. Aerosol Sci. Tech. 47(11), 1205-1214. http://dx.doi.org/10.1080/02786826.2013.829908.

Timko, M.T., Yu, Z., Onasch, T.B., Wong, H.W., Miake-Lye, R.C., Beyersdorf, A.J., Anderson, B.E., Thornhill, K.L., Winstead, E.L., Corporan, E., DeWitt, M.J., Klingshirn, C.D., Wey, C., Tacina, K., Liscinsky, D.S., Howard, R., Bhargava, A., 2010. Particulate Emissions of Gas Turbine Engine Combustion of a Fischer−Tropsch Synthetic Fuel. Energ. Fuel. 24(11), 5883-5896. http://dx.doi.org/10.1021/ef100727t.

Ukrainec, A., Haykin, S., McGregor, J., 1989. In A neural network nonlinear predictor, International 1989 Joint Conference on Neural Networks. IEEE, Washington, DC, USA.

Undavalli, V.K., Khandelwal, B., 2021. Chapter 5 - Impact of alternative fuels and fuel properties on PM emissions, Aviation Fuels. Academic Press. https://doi.org/10.1016/B978-0-12-818314-4.00012-1.

Voigt, C., Kleine, J., Sauer, D., Moore, R.H., Brauer, T., Le Clercq, P., Kaufmann, S., Scheibe, M., Jurkat-Witschas, T., Aigner, M., Bauder, U., Boose, Y., Borrmann, S., Crosbie, E., Diskin, G.S., DiGangi, J., Hahn, V., Heckl, C., Huber, F., Nowak, J.B., Rapp, M., Rauch, B., Robinson, C., Schripp, T., Shook, M., Winstead, E., Ziemba, L., Schlager, H., Anderson, B.E., 2021. Cleaner burning aviation fuels can reduce contrail cloudiness. Commun. Earth Environ. 2(1), 114. http://dx.doi.org/10.1038/s43247-021-00174-y.

Wayson, R.L., Fleming, G.G., Iovinelli, R., 2009. Methodology to Estimate Particulate Matter Emissions from Certified Commercial Aircraft Engines. J. Air Waste Manage. 59(1), 91-100. http://dx.doi.org/10.3155/1047-3289.59.1.91.

Wilkerson, J.T., Jacobson, M.Z., Malwitz, A., Balasubramanian, S., Wayson, R., Fleming, G., Naiman, A.D., Lele, S.K., 2010. Analysis of emission data from global commercial aviation: 2004 and 2006. Atmos. Chem. Phys. 10(13), 6391-6408. http://dx.doi.org/10.5194/acp-10-6391-2010.

Yim, S.H.L., Lee, G.L., Lee, I.H., Allroggen, F., Ashok, A., Caiazzo, F., Eastham, S.D., Malina, R., Barrett, S.R.H., 2015. Global, regional and local health impacts of civil aviation emissions. Environ. Res. Lett. 10(3), 034001. http://dx.doi.org/10.1088/1748-9326/10/3/034001.

Yim, S.H.L., Stettler, M.E.J., Barrett, S.R.H., 2013. Air quality and public health impacts of UK airports. Part II: Impacts and policy assessment. Atmospheric Environ. 67, 184-192. http://dx.doi.org/10.1016/j.atmosenv.2012.10.017.

Zhang, X.L., Chen, X., Wang, J., 2019. A number-based inventory of size-resolved black carbon particle emissions by global civil aviation. Nat. Commun. 10(1), 534. http://dx.doi.org/10.1038/s41467-019-08491-9.